

¹R. Smoluchowski, *Colloque Ampère XV* (North-Holland, Amsterdam, 1969), p. 120.

²S. Kapphan and F. Lüty, International Symposium on Color Centers, Rome, 1968 (unpublished).

³K. Füssgaenger, *Phys. Status Solidi* **36**, 645 (1969).

⁴J. A. D. Matthew, Cornell University Material Science Division Report No. 373, 1965 (unpublished).
W. D. Wilson, R. D. Hatcher, G. J. Dienes, and R. Smoluchowski, *Phys. Rev.* **161**, 888 (1967).

⁵R. J. Quigley and T. P. Das, *Phys. Rev.* **164**, 1185 (1967).

⁶G. Benedek and G. F. Nardelli, *J. Chem. Phys.* **48**, 5242 (1968).

⁷G. Baldini, A. Jean, and G. Spinolo, *Phys. Status Solidi* **25**, 557 (1968).

⁸M. Piccirilli and G. Spinolo (unpublished).

⁹P. Weber and P. Nette, *Phys. Letters* **20**, 495 (1966).

PHYSICAL REVIEW B

VOLUME 4, NUMBER 4

15 AUGUST 1971

Intermediate Coupling Theory: Padé Approximants for Polarons*

Ping Sheng[†] and John D. Dow[‡]

Joseph Henry Laboratories of Physics, Princeton University, Princeton, New Jersey 08540

(Received 14 January 1971; revised manuscript received 22 March 1971)

A general method is presented for obtaining an accurate intermediate-coupling theory from weak- and strong-coupling perturbation theory. The method uses two-point Padé approximants to extrapolate (low-order) expansions about the weak- and the strong-coupling limits into the intermediate-coupling regime. The method is used to evaluate the ground-state energy and effective mass of the polaron with gratifying success. In addition, the weak-coupling perturbation theory of the polaron dispersion relation, ground-state energy, and effective mass are extended to fourth, sixth, and fourth order, respectively. A scheme based on two-point Padé approximants is used to obtain an optimal polaron dispersion relation.

I. INTRODUCTION

A typical problem of theoretical physics is the accurate evaluation of perturbation expansions in the intermediate-coupling regime; that is, for strengths of the perturbation which are not small enough to guarantee either convergence of the series or an accurate asymptotic approximation to it. In some cases it is possible to obtain perturbation expansions about the weak- and strong-coupling limits, but there is no simple scheme for obtaining accurate perturbation expansions for intermediate values of the coupling constant. In this paper we present a systematic procedure for obtaining intermediate-coupling expansions, and we use this procedure to obtain adequate expressions for the ground-state energy and the effective mass of a polaron—an electron interacting with the longitudinal-optical-phonon mode of a polar insulator.¹⁻³

The procedure for evaluating intermediate-coupling perturbations consists of obtaining a two-point Padé approximant⁴⁻⁶ to both the weak-coupling⁷ ($\alpha = 0$) and the strong-coupling⁸ ($\alpha = \infty$) expansions. This procedure is complementary to existing variational theories of intermediate coupling⁹⁻¹⁴ in that it provides a simple (albeit unphysical) method for deducing intermediate-coupling results from a knowledge of the weak- and strong-coupling expansions. In principle the two-

point Padé method, carried to sufficiently high order, should be capable of attaining the intermediate-coupling results to any degree of accuracy. While the variational methods require physical insight in the choice of trial functions, the Padé method only requires labor in evaluating the power series about $\alpha = 0$ and $\alpha = \infty$. Although the variational method can, for example, guarantee that a calculated energy is an upper bound of the true energy; the Padé method makes no such claims,¹⁵ but should be able to locate singularities in the perturbation expansion as a function of coupling constant. In addition, the Padé method is even capable of suggesting the nature of the singularities (i.e., poles, cuts, etc.).

The two-point Padé method is, of course, an extension of the one-point Padé approximant method which has found considerable success in various branches of physics.¹⁶ Such Padé approximants have been used in the study of interacting hard-core bosons,¹⁷ in investigations of Regge-pole trajectories,¹⁸ in phase-transition theories (to predict critical behaviors),¹⁹ and in theories of the anharmonic oscillator,²⁰ van der Waals interactions in helium,²¹ oscillator strengths,^{20,22} and exciton migration.²³ In all of these theories the essential role of the Padé approximant is to provide a method for analytically continuing power series; in all cases the Padé approximant seems to provide an almost unbelievably good representation of the

analytic continuation—even when the perturbation series itself diverges or when there are singularities in the function being continued!

In Sec. II of this paper we discuss one- and two-point Padé approximants as a formal device for estimating the analytic continuations of power series. Section III is devoted to an application of two-point Padé approximants to calculate the ground-state energy and effective mass of the polaron. Section IV contains an attempt to obtain the polaron-dispersion relation using Padé methods, and Sec. V summarizes our results.

II. PADÉ APPROXIMANTS

A. One-Point Padé Approximants

The one-point $[M, N]$ Padé approximant $P_f([M, N]; Z)$ to the power series

$$f(Z) = f_0 + f_1 Z + f_2 Z^2 + \dots \tag{2.1}$$

is the ratio of polynomials of orders N and M which exactly reproduces the first $M + N + 1$ terms of the series¹⁶

$$P_f([M, N]; Z) = \frac{a_0 + a_1 Z + a_2 Z^2 + \dots + a_N Z^N}{1 + b_1 Z + \dots + b_M Z^M} = f_0 + f_1 Z + \dots + f_{N+M} Z^{N+M} + O(Z^{N+M}). \tag{2.2}$$

Here $O(Z^L)$ means terms of order Z^L or higher. The coefficients a_n and b_m are uniquely determined by the specification of the f_i 's, and the Padé approximant can be written in terms of the coefficients f_i ($i = 0, 1, 2, \dots, N + M$) as a ratio of determinants⁴

$$P_f([M, N]; Z) = \frac{\begin{vmatrix} f_{N-M+1} & \dots & f_{N+1} \\ \vdots & & \vdots \\ f_N & & f_{M+N} \\ \sum_{j=M}^N f_{j-M} Z^j & \dots & \sum_{j=0}^N f_j Z^j \end{vmatrix}}{\begin{vmatrix} f_{N-M+1} & \dots & f_{N+1} \\ \vdots & & \vdots \\ f_N & & f_{M+N} \\ Z^N & \dots & 1 \end{vmatrix}}, \tag{2.3}$$

where $f_j = 0$ if $j < 0$.

The primary advantages of a Padé approximant over a power-series representation of a function are (i) the domain of convergence of the Padé approximant is not necessarily a circle and generally is much larger than the circle of convergence of the series; (ii) the Padé approximant affords

a simple prescription for analytic continuation of the power series (2.1) into regions outside its circle of convergence; (iii) the Padé approximant can simulate the behavior of $f(Z)$ near its singularities with one or more poles; for example, a function with a branch line could be adequately represented by a Padé approximant with several poles on the cut. In fact, by examining the $[N, N]$ Padé approximant to a function for increasing N , one can often guess many facts about the positions and the natures of the singularities of the function.

For example, the series $g(Z) = 1 + Z + Z^2 + \dots$ diverges for $|Z| > 1$. The $[1, 1]$ Padé approximant to $g(Z)$ is

$$P_g([1, 1]; Z) = 1/(1 - Z) \tag{2.4}$$

and provides the exact analytic continuation of $g(Z)$ throughout all space, even where the series is divergent.

As another example, consider $h(Z) = \tan Z$, which is an analytic function of Z except at $Z = \pm \frac{1}{2}(2n - 1)\pi$ ($n = 1, 2, \dots$), where $\tan Z$ has poles. The power-series expansion of $\tan Z$ is

$$\tan Z = Z + \frac{Z^3}{3} + \frac{2}{15} Z^5 + \frac{17}{315} Z^7 + \frac{62}{2835} Z^9 + \dots \tag{2.5}$$

and converges for $|Z| < \frac{1}{2}\pi$. Factoring out one power of Z , we form the $[1, 1]$ Padé approximant to $\tan Z$ in terms of Z^2 :

$$P_{\tan}([1, 1]; Z^2) = Z(15 - Z^2)/(15 - 6Z^2) \tag{2.6}$$

which has poles at ± 1.581 , less than 1% different from the exact values $\pm \frac{1}{2}\pi$! This very simple approximation represents $\tan Z$ amazingly well for $|Z| < 0.8\pi$ (see Fig. 1). To improve on this, we construct the $[2, 2]$ Padé approximant to $\tan Z$,

$$P_{\tan}([2, 2]; Z^2) = Z \frac{63 - 7Z^2 + \frac{1}{15}Z^4}{63 - 28Z^2 + Z^4}, \tag{2.7}$$

which has poles at $Z = \pm 1.569$ and ± 5.05 (compared with the poles of $\tan Z$ at $\pm \frac{1}{2}\pi = \pm 1.5708$ and $\pm \frac{3}{2}\pi = \pm 4.7124$). Again the Padé approximant reproduces the function $\tan Z$, including its singularities, with amazing faithfulness, far beyond the circle of convergence of the power series²⁴ (see Fig. 1) even though all the information used in determining $P_{\tan}([2, 2]; Z^2)$ comes from near $Z = 0$.

The formal properties of Padé approximants and their regions of convergence are only poorly understood. There are some theorems which apply to Stieltjes series, as well as a general conjecture that the $[N, N]$ Padé approximant converges to the function (as N approaches infinity) almost everywhere except around poles, cuts, and essential singularities of the function.⁴ This latter conjecture has been verified for many examples, and it probably is true for most, if not all, functions of phys-

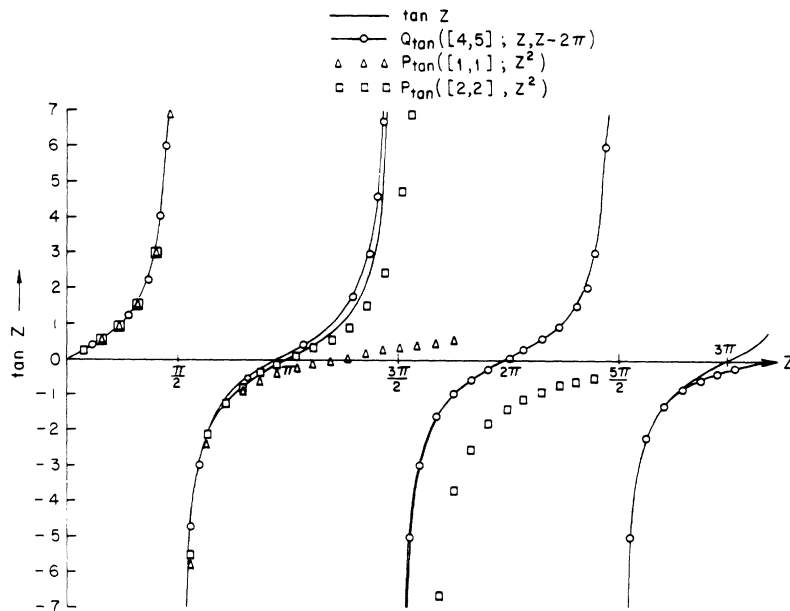


FIG. 1. Padé approximants to $\tan z$ as a function of z . Solid line: $\tan z$; line with circles: two-point ($z=0$ and $z=2\pi$) [4, 5] Padé approximant; triangles: one-point ($z=0$) [1, 1] Padé approximant in z^2 ; squares: one-point ($z=0$) [2, 2] Padé approximant in z^2 .

ical relevance, although no proof of the conjecture exists.

B. Two-Point Padé Approximants

The one-point Padé approximant to a function is defined as the ratio of polynomials which reproduces the first several terms of the Taylor expansion of the function about $Z=0$. Similarly a two-point Padé approximant may be defined as a ratio of polynomials whose coefficients are fixed so that the approximant reproduces the first several terms in expansions about *both* $Z=0$ and some other point $Z=Z_0$ (where Z_0 may be infinity). The advantages of the two-point approximants over the one-point variety are illustrated for the function $\tan Z$ in Fig. 1. The one-point approximant (squares in Fig. 1) to $\tan Z$, $P_{\tan}([2, 2]; Z^2)$, provides an adequate representation of the function for $|Z| < \pi$ using the facts that

$$\tan Z = Z + \frac{Z^3}{3} + \frac{2}{15} Z^5 + \frac{17}{315} Z^7 + \frac{62}{2835} Z^9 + O(Z^{11}). \quad (2.8)$$

The two-point Padé approximant²⁵ uses the same amount of information with more than half coming from near $Z=0$ and the rest coming from near $Z=2\pi$:

$$\tan Z = Z + \frac{1}{3} Z^3 + \frac{2}{15} Z^5 + O(Z^7), \quad (2.9a)$$

$$\tan Z = (Z - 2\pi) + \frac{1}{3} (Z - 2\pi)^3 + O((Z - 2\pi)^5). \quad (2.9b)$$

The two-point Padé approximant represents $\tan Z$ amazingly well for $0 \leq Z \leq 2\pi$ [even though both series (2.9a) and (2.9b) diverge for $\frac{1}{2}\pi < Z < \frac{3}{2}\pi$] and

is even adequate over the entire range $-\frac{1}{2}\pi < Z < 3\pi$!

The example of $\tan Z$ illustrates how the Padé approximants provide a simple but accurate way of interpolating a function over a broad range of values, given only the value of the function and its first few derivatives at two points. Although a special version of two-point Padé approximants has been studied previously,⁵ the advantages of the two-point Padé method of analytic continuation do not seem to be widely recognized. Indeed n -point Padé approximants (with $n \geq 2$) can provide simple interpolation schemes based on the values of the derivatives of a function as well as the function, and may find extensive application in numerical analysis,^{26, 27} phase-transition theory,²⁸ and energy-band theory.²⁹

The two-point Padé approximants most useful in physics generally involve expansions about $Z=0$ and $Z=\infty$, where Z is some coupling constant or expansion parameter. For example, the ground-state energy of a polaron, $E_0(\alpha)$, can be evaluated by perturbation theory for small values of the electron-phonon coupling constant α and by variational methods for the strong-coupling limit $\alpha \rightarrow \infty$; it is possible to estimate the value of $E_0(\alpha)$ for intermediate values of α (i.e., $\alpha \geq 1$) by fitting the expansions of $E_0(\alpha)$ about $\alpha=0$ and $\alpha=\infty$ to a two-point Padé approximant. Therefore, a knowledge of weak- and strong-coupling expansions leads, via the two-point Padé method, to a knowledge of intermediate-coupling theory.

The general mathematical problem is as follows: Given a function $f(Z)$, find $Q([M, M+n]; Z, Z^{-1})$, the ratio of polynomials of order $M+n$ and M , respec-

tively, such that

$$\lim_{Z \rightarrow 0} |Q(Z) - f(Z)| = O(Z^{\lambda+1}),$$

$$\lim_{Z \rightarrow \infty} |Q(Z) - f(Z)| = O(Z^{-\lambda-1}). \tag{2.10}$$

Let $Q(Z)$ be given by

$$Q([M, M+n]; Z, Z^{-1}) = \frac{a_0 + a_1 Z + a_2 Z^2 + \dots + a_{M+n} Z^{M+n}}{1 + b_1 Z + b_2 Z^2 + \dots + b_M Z^M}, \tag{2.11}$$

and suppose that $f(Z)$ has the expansions about $Z=0$ and $Z=\infty$, respectively,

$$f(Z) = f_0 + f_1 Z + f_2 Z^2 + \dots + f_l Z^l + \dots + O(Z^{l+1}) \tag{2.12a}$$

and

$$f(Z) = \gamma_n Z^n + \gamma_{n-1} Z^{n-1} + \dots + \gamma_{-\lambda} Z^{-\lambda} + O(Z^{-\lambda-1}). \tag{2.12b}$$

Note that we have $2M+n=l+\lambda+1$, and that n may be any integer. Equations (2.10)–(2.12) lead to the following equations:

$$a_0 + a_1 Z + \dots + a_{M+n} Z^{M+n} = (1 + b_1 Z + \dots + b_M Z^M) \times (f_0 + f_1 Z + \dots + f_l Z^l) + O(Z^{l+1}), \tag{2.13a}$$

$$a_0 Z^{-M-n} + a_1 Z^{-M-n+1} + \dots + a_{M+n} = (1 + b_1 Z + \dots + b_M Z^M) \times (\gamma_n Z^M + \gamma_{n-1} Z^{M-1} + \dots + \gamma_{-\lambda} Z^{M-n-\lambda}) + O(Z^{M-n-\lambda-1}). \tag{2.13b}$$

Equating coefficients of equal powers of Z in Eqs. (2.13a) and (2.13b), we obtain a set of linear equations for the unknowns a_i and b_j ($i=0, 1, 2, \dots, M+n$; $j=1, \dots, M$) as functions of the known coefficients f_k and γ_p ($k=0, 1, \dots, l$; $p=n, n-1, \dots, -\lambda$),

$$a_\nu = \sum_{\mu=0}^{\nu} f_\mu b_{\nu-\mu} \quad \text{for } \nu=0, 1, \dots, l \tag{2.14a}$$

and

$$a_{M+n-\nu} = \sum_{\mu=0}^{\nu} b_{M-\mu} \gamma_{n-\nu+\mu} \quad \text{for } \nu=0, 1, \dots, \lambda. \tag{2.14b}$$

Here we take $b_0=1$ and $a_i=0$ for $i>M+n$ or $i<0$ and $b_j=0$ for $j>M$ or $j<0$.

The set of linear equations (2.14a) and (2.14b) can

be solved by standard methods for the coefficients of the Padé approximant.

III. POLARON GROUND-STATE ENERGY AND EFFECTIVE MASS: QUALITATIVE ASPECTS

A polaron is a conduction electron interacting with the electric field of longitudinal-optical phonons in a polar crystal.¹⁻³ Such an interaction is the dominant electron-phonon interaction in polar crystals, and the Hamiltonian for the system of extra conduction electron plus longitudinal optical phonons plus electron-phonon interaction is described (in a dielectric continuum approximation) by the Fröhlich Hamiltonian³⁰

$$H = \sum_{\mathbf{k}} \frac{\hbar^2 k^2}{2m} c_{\mathbf{k}}^\dagger c_{\mathbf{k}} + \hbar\Omega \sum_{\mathbf{q}} (a_{\mathbf{q}}^\dagger a_{\mathbf{q}} + \frac{1}{2}) + H_1. \tag{3.1}$$

Here the interaction Hamiltonian H_1 is

$$H_1 = i\hbar\Omega \left(\frac{4\pi\alpha}{V} \right)^{1/2} \left(\frac{\hbar}{2m\Omega} \right)^{1/4} \sum_{\mathbf{q}} \frac{1}{|\mathbf{q}|} (a_{\mathbf{q}}^\dagger - a_{-\mathbf{q}}) \rho_{-\mathbf{q}}, \tag{3.2}$$

where Ω is the optical-phonon frequency, $\rho_{\mathbf{q}} = \sum_{\mathbf{k}} c_{\mathbf{k}-\mathbf{q}}^\dagger c_{\mathbf{k}}$ is the second-quantized electron density operator, and

$$\alpha = \frac{e^2}{2} \left(\frac{1}{\epsilon_\infty} - \frac{1}{\epsilon_0} \right) \left(\frac{2m}{\Omega\hbar^3} \right)^{1/2}$$

is the dimensionless polaron coupling constant. Here e is the charge of the electron, m is the conduction-band mass, ϵ_0 and ϵ_∞ are the static and optical dielectric constants of the solid, and $a_{\mathbf{q}} (a_{\mathbf{q}}^\dagger)$ is an operator which destroys (creates) a longitudinal-optical phonon of wave vector \mathbf{q} .

There are two limits in which an approximate solution of the Schrödinger equation for the Hamiltonian (3.1) can be obtained: the weak-coupling limit ($\alpha \ll 1$),⁷ and the strong-coupling extreme ($\alpha \gg 1$).^{8, 14} Physically a weak-coupling polaron is an electron moving through the crystal while carrying approximately $\frac{1}{2}\alpha$ virtual phonons with it. The weak-coupling polaron moves coherently through the crystal, although its effective mass is somewhat greater than the electron's band mass on account of the lattice polarization it drags along with it. In contrast, the strong-coupling polaron hops incoherently from lattice site to lattice site with the electron's phase completely destroyed by many collisions with phonons. In moving, the strong-coupling polaron must carry the complete lattice distortion with it; therefore its effective mass is very large (typically equal to an ionic mass).

The ground-state energy E_0 and effective mass m^* of the polaron have been evaluated^{1, 2} (a) by a weak-coupling ($\alpha \ll 1$) perturbation expansion^{7, 31}; (b) by the weak-coupling Tamm-Dancoff¹ and improved Tamm-Dancoff approximations³²; (c) by

strong-coupling ($\alpha \gg 1$) variational calculations^{3,8,33}; (d) by variational intermediate-coupling theories^{9,10}; and (e) by Feynman's variational-path integral method (for all α).¹⁴

The perturbation results, of course, are only valid for small-coupling constants and for energies well below the one-phonon threshold. The Tamm-Dancoff approximation is a variational calculation using a trial wave function which contains only zero- and one-phonon states:

$$\Phi_{\mathbf{k}} = (u_{\mathbf{k}} c_{\mathbf{k}}^{\dagger} + \sum_{\mathbf{q}} v_{\mathbf{k},\mathbf{q}} c_{\mathbf{k}-\mathbf{q}}^{\dagger} a_{\mathbf{q}}^{\dagger} | 0 \rangle). \quad (3.3)$$

The variational parameters $u_{\mathbf{k}}$ and $v_{\mathbf{k},\mathbf{q}}$ are determined by minimizing the energy. Even though the Tamm-Dancoff approximation is a weak-coupling one-phonon approximation, it should be especially good in the vicinity of the phonon-emission threshold: It treats the strong mixing between the zero- and one-phonon states exactly as is equivalent to diagonalizing the polaron Hamiltonian in the subspace of Hilbert space spanned by the zero- and one-phonon states. [In terms of diagrams,³⁴ the self-energy (defined by the integral equation of Fig. 2) is given in the Tamm-Dancoff approximation by Fig. 3.] However, the Tamm-Dancoff approximation does not include the mixing of many-phonon states, and therefore should not be appreciably better than second-order perturbation theory in predicting the polaron energy and mass near $k=0$.^{1,35} The improved Tamm-Dancoff approximation is equivalent to including all the nested-diagram (Fig. 4) many-phonon states in the evaluation of the electron's self-energy. However, the nested diagrams are not the most important ones, and become relatively less important than the omitted crossing diagrams in higher orders. For example, even in fourth order the nested diagram [Fig. 5(a)] is only slightly larger in magnitude than the crossing diagram [Fig. 5(b)] which has the same (negative) sign; but the sum of the nested and the crossing diagram more than cancels the positive contribution of the reducible diagram [Fig. 5(c)] resulting in a negative fourth-order en-

$$\begin{array}{c} \begin{array}{ccc} \parallel & = & \parallel \\ \parallel & & \parallel \end{array} \\ G = G^{\circ} + G^{\circ} \Sigma G \end{array}$$

FIG. 2. Integral equation for the polaron Green's function G in terms of the free-electron Green's function G° and the polaron self-energy Σ .

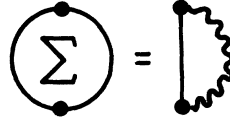


FIG. 3. Tamm-Dancoff approximation to the polaron self-energy. A wiggly line is a free-phonon propagator.

ergy. The various strong-coupling results are based on variational methods using trial wave functions of a localized nature, and therefore are not capable of describing the weak- and the intermediate-coupling regimes. The intermediate-coupling theory is based on a canonical transformation^{31,36} and a variational determination of the polaron wave function and energy; still, the intermediate-coupling trial wave function implicitly contains the physical assumption of reasonably weak coupling and a delocalized large polaron. Only the Feynman theory hopes to describe weak-, intermediate-, and strong-coupling polarons.¹⁴ But it is based on a path-integral formulation which requires the numerical evaluation of a two-parameter expression for the ground-state energy and the effective mass.

The two-point Padé approximant scheme should provide an easy method for incorporating all the good features of the various approximation schemes into simple expressions for E_0 and m^* . In the remaining parts of this section, we shall first test the two-point Padé approximant method by determining how well the Padé approximant method (fitted to the Feynman expressions for E_0 and m^*) describes the Feynman results. By this procedure we shall demonstrate that the two-point Padé method provides a very accurate representation of the Feynman calculation. Therefore the Padé method, when applied to the perturbation results, can be expected to provide an equally good representation of the actual polaron energy and mass—especially for very weak and very strong coupling where the Feynman formulas are known to disagree with fourth- and higher-order perturbation theory. Second, we shall extend the weak-coupling perturbation theory to sixth order for E_0 and fourth order for (m/m^*) ; and finally we shall obtain a two-point Padé approximant to these higher-order perturbation expansions and to the strong-coupling expansions.³⁷

In obtaining a Padé approximant to Feynman's expressions³⁸ for E_0 and m^* , we first expand those

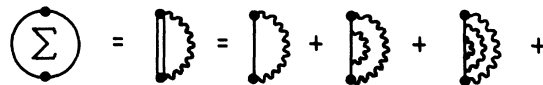


FIG. 4. Whitfield-Puff approximation to the polaron self-energy.

expressions in the weak- and strong-coupling limits:

$$\left. \frac{E_0}{\hbar\Omega} \right|_{\text{Feyn}} = \begin{cases} -\alpha - (0.98 \times 10^{-2}) \alpha^2 \\ -(0.6 \times 10^{-3}) \alpha^3 + O(\alpha^4) \\ -0.106 \alpha^2 - 2.83 + O(\alpha^{-2}), \end{cases} \quad (3.4)$$

$$\left. \frac{m^*}{m} \right|_{\text{Feyn}} = \begin{cases} 1 + \frac{1}{8} \alpha + \frac{1}{40} \alpha^2 + O(\alpha^3) \\ 0.02 \alpha^4 - 1.01 \alpha^2 + O(\alpha). \end{cases} \quad (3.5)$$

With this information we can fit Feynman's E_0 with a [2, 4] Padé approximant:

$$\left. \frac{E_0}{\hbar\Omega} \right|_{\text{Feyn}} \cong \frac{-\alpha - 0.139653 \alpha^2 - 0.013764 \alpha^3 - 0.001260 \alpha^4}{1 + 0.129853 \alpha + 0.011891 \alpha^2}. \quad (3.6)$$

To fit m^*/m , we factor out the behavior at infinity and then fit a [2, 2] Padé approximant to the series $1 + \frac{1}{8} \alpha + 1.035 \alpha^2 - 0.02 \alpha^4$. The result is

$$\left. \frac{m^*}{m} \right|_{\text{Feyn}} \cong 0.02 \alpha^4 - 1.01 \alpha^2 + \frac{1.128863 \alpha^2 + 0.175204 \alpha + 1.071225}{0.0207 \alpha^2 - 0.003333 \alpha + 1.071225}. \quad (3.7)$$

The results of the Feynman calculation and the Padé approximant to it are displayed in Figs. 6 and 7. Note that the differences between the exact Feynman expressions and the approximants to them differ *at most* by 6–7% and 21% for E_0 and $\ln m^*$, respectively. In general, the Padé approximants provide a very good description of the ground-state energy and mass of the Feynman polaron. Therefore we feel justified in attempting to obtain an improved systematic weak- and intermediate-coupling theory of polarons using the two-point Padé approximant method. We emphasize that the advantage of such a Padé approximant scheme is that it can give an intermediate-coupling theory which, in principle, is exact; that is, as the order of the approximant is increased, the approximants converge to the exact results. Therefore, an arbitrarily accurate intermediate-coupling theory can be achieved by simply evaluating the weak- and strong-coupling expansions to sufficiently high order.

In order to compare the two-point Padé method based on perturbation theory with the Feynman result, we first evaluate the weak-coupling perturbation expansions to sixth and fourth orders for E_0 and m^* , respectively. In fourth order, there are

$$\left. \frac{E_0}{\hbar\Omega} \right|_{\text{pert}} \cong \frac{-\alpha - 0.103529 \alpha^2 - 0.009287 \alpha^3 + 0.000093 \alpha^4}{1 + 0.087609 \alpha - 0.000873 \alpha^2} \quad (3.11)$$

and

$$\left. \frac{m^*}{m} \right|_{\text{pert}} \cong 0.02 \alpha^4 - 1.01 \alpha^2 + \frac{1.065653 \alpha^2 + 0.168395 \alpha + 1.030367}{0.020301 \alpha^2 - 0.003333 \alpha + 1.030367}. \quad (3.12)$$

The [2, 4] approximant (3.11) to the ground-state energy has a pole near $\alpha \approx 400$ which is due to the large coefficient of the α^3 term in perturbation

three contributions to the polaron energy, indicated in standard diagram notation³⁴ in Fig. (5). The contributions of the diagrams are given in Table I.

The details of the fourth-order calculation are given in Appendix B; a similar sixth-order calculation is also presented in Appendix B. The resulting weak-coupling expansions of the ground-state energy and effective mass of the polaron are³⁹

$$\left. \frac{E_0}{\hbar\Omega} \right|_{\text{pert}} = -\alpha - 0.01592 \alpha^2 - 0.008765 \alpha^3 + \dots \quad (3.8)$$

and

$$\left. \frac{m^*}{m} \right|_{\text{pert}} = 1 - \frac{1}{8} \alpha + 0.02263 \alpha^2 + \dots \quad (3.9)$$

Two-point Padé approximants can be constructed to fit these results [Eqs. (3.8) and (3.9)], Allcock's strong-coupling values³ of E_0 (calculated using the theory of Bogoliubov and Tyablikov⁴⁰)

$$\left. \frac{E_0}{\hbar\Omega} \right|_{\text{pert}} = -0.1088 \alpha^2 - 2.83, \quad (3.10)$$

and Feynman's strong-coupling expansion [Eq. (3.5)] for m^* . The results are displayed in Figs. 6 and 7,

theory. While it is possible that this pole is signaling a singularity in $E_0(\alpha)$, the perturbation calculation would have to be carried to higher order

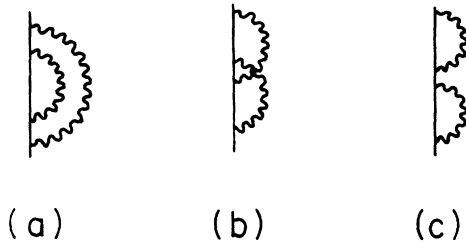


FIG. 5. Diagrams contributing to the polaron energy in fourth-order perturbation theory: (a) nested diagram; (b) crossing diagram; (c) reducible diagram.

and a $[3, 5]$ approximant determined before one could have any confidence in predicting such a singularity. Furthermore, strong-coupling theory is generally valid for $\alpha \gtrsim 20$, so that if $E_0(\alpha)$ has a singularity it should occur for α less than 20; therefore it is most likely that the pole is simply a result of terminating the perturbation expansion after terms of α^3 . In order to improve the Padé estimate of $E_0(\alpha)$ for α less than 20, we have evaluated the $([1, 3]; \alpha, \alpha - 20)$ Padé approximant⁴¹

to $E_0(\alpha)$ [Fig. 6(b)] by expanding the strong-coupling theory about $\alpha = 20$. These results are also displayed in Figs. 6 and 7 and are presented in tabular form in Tables II and III. The difference between the approximants to the Feynman curves (line of \times) and the Feynman curves (dotted lines with F) is a measure of the error in the Padé approximants to the perturbation series.

Looking at Figs. 6 and 7 we conclude that the two-point Padé approximant method provides an astonishingly accurate scheme for determining the intermediate-coupling energy and mass of the polaron. From Fig. 6, we deduce that the two-point Padé method describes the ground-state energy to within a few percent and that it is far superior to perturbation theory, Tamm-Dancoff theory, and the intermediate-coupling theory of Lee and Pines. Only the Feynman theory seems to describe the intermediate-coupling regime well, and it fails to obtain a sufficiently low ground-state energy at weak coupling (Fig. 8) and at strong coupling [compare Eq. (3.4) and Eq. (3.10)]. For the effective mass, only the Feynman calculation gives reasonable answers in both the weak- and strong-

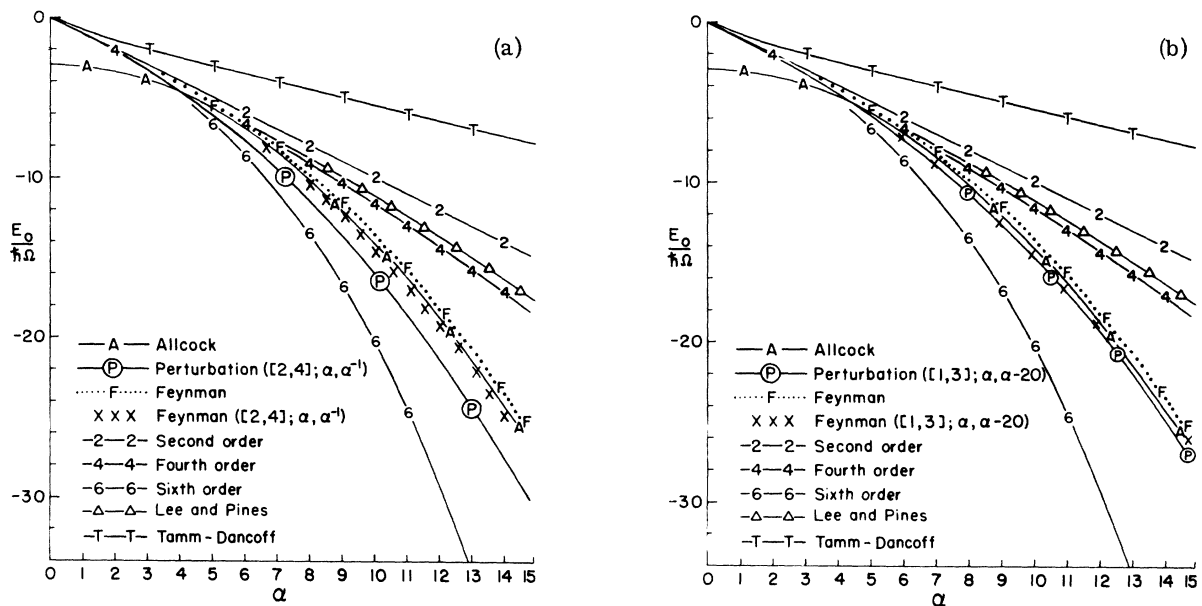


FIG. 6. (a) Ground-state energy of the polaron, E_0 (in units of optical-phonon energy $\hbar\Omega$), as a function of polaron coupling constant α . Second-, fourth-, and sixth-order perturbation theory are denoted by the lines labeled 2, 4, and 6, respectively. The dotted line with F represents Feynman's variational calculation (Ref. 3); the \times represents the two-point ($\alpha = 0$ and $\alpha = \infty$) Padé approximant to Feynman's calculation. The two-point Padé approximant to sixth-order weak-coupling perturbation theory and strong-coupling variational theory is denoted by a solid line with circled P. Allcock's strong-coupling variational result is denoted by a solid line with A. The Tamm-Dancoff approximation is denoted by T (Ref. 1); and the intermediate-coupling results for Lee and Pines (Ref. 10) is denoted by triangles. Note that (i) the Padé approximant (\times) to Feynman theory fits that theory (F) quite well; (ii) the Padé approximant to perturbation theory (P) is in good agreement with Feynman's theory; and (iii) the Padé approximants seem to give more plausible values of E_0 than the intermediate-coupling theory of Lee and Pines. (b) Ground-state energy of the polaron E_0 as a function of coupling constant α . The notation here is the same as in (a). The two-point Padé approximants in this figure are fitted to weak- and strong-coupling expansions around $\alpha = 0$ and $\alpha = 20$, respectively.

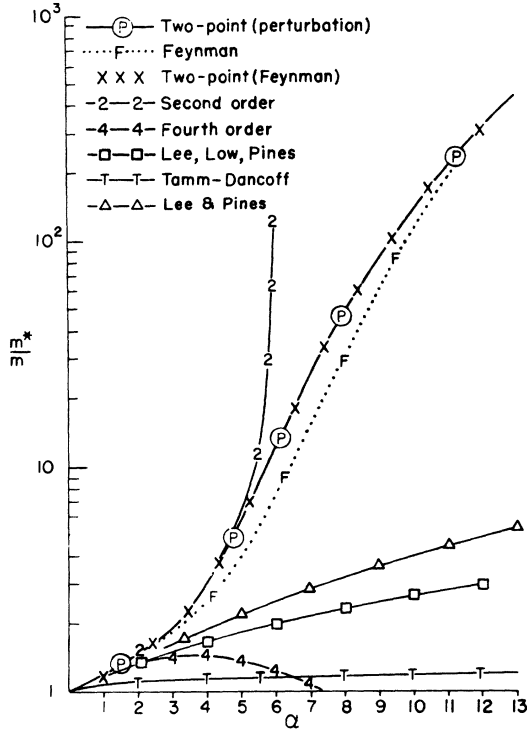


FIG. 7. Polaron effective mass as a function of coupling constant α . Second- and fourth-order perturbation calculation are denoted by solid lines labeled 2 and 4, respectively. The dotted line with F represents Feynman's variational calculation; the \times represent the two-point Padé approximant to Feynman's weak- and strong-coupling expansions. The two-point Padé approximant to fourth-order perturbation theory and strong-coupling variational theory is denoted by a solid line with circled P. (Note that it nearly coincides with the Padé approximant to Feynman theory.) The triangles and the squares denote the intermediate-coupling results of Lee and Pines and of Lee, Low, and Pines, respectively. The solid line with T represents the Tamm-Dancoff approximation.

coupling limits, and the Padé approximant to Feynman theory (which differs only slightly for $\alpha \gtrsim 3$ from the Padé approximant to perturbation theory) fits it quite well. Again, in the weak-coupling regime, the Padé approximant which reproduces perturbation theory is superior to Feynman's calculation (Fig. 9).

In view of the remarkable similarity between the Padé approximants to E_0 and m^* and the Feynman results, we believe that E_0 and m^* are continuous functions of the coupling strength α . Had there been a discontinuity in either E_0 or m^* , the Padé approximant would have tried to simulate the singularity, and there is no evidence of such a singularity in Figs. 6 and 7. Therefore, we believe that the Padé approximants indicate that the polaron wave function changes continuously and smoothly

as the coupling strength is increased; not discontinuously and abruptly (for $\alpha \approx 6$), as suggested recently.^{41a} Therefore electron self-trapping via interaction with the longitudinal-optical phonons should not occur.⁴²

The astounding conclusion of these calculations is that a very accurate intermediate-coupling theory can be obtained simply by first evaluating the first few terms in the weak- and the strong-coupling theories and then joining the two limits using two-point Padé approximants. The success of the method for intermediate-coupling polaron theory is remarkable. The method accurately describes the polaron ground-state energy E_0 and effective mass m^* in the (approximate) Feynman theory, and seems to predict m^* and E_0 with comparable accuracy without having to resort to either displaced oscillator transformations or path integrals.

IV. POLARON DISPERSION RELATION $E(k)$

In theories of the transport and the optical properties of polarons, it is necessary to know the complete dispersion relation $E(k)$ as well as the ground-state energy and effective mass. In this section, we review some existing theories of the polaron dispersion relation and use Padé approximants to obtain a "best" dispersion relation using the best parts of the various theories. Our results should be particularly useful for weak to intermediate coupling.

Due to the strong mixing of one-electron zero-phonon states with one-electron one-phonon states near $k = (2m\Omega/\hbar)^{1/2}$, second-order perturbation theory attempts to simulate a phonon-emission threshold there, but fails by obtaining a cusped shape (see Fig. 10) rather than the expected threshold behavior: The second-order energy is

$$E(\alpha, k) = \frac{\hbar^2 k^2}{2m} - \frac{\alpha \hbar \Omega}{k(\hbar/2m\Omega)^{1/2}} \times \sin^{-1} \frac{k(\hbar^2/2m)^{1/2}}{(\hbar\Omega - \hbar^2 k^2/2m)^{1/2}}. \quad (4.1)$$

In an attempt to improve on some of the shortcomings of second-order perturbation theory, we have evaluated the fourth-order energy using Ray-

TABLE I. Contributions of the various terms of fourth-order perturbation theory to E_0 and m/m^* .

	Contribution to $E_0/\hbar\Omega$	Contribution to m/m^*
Fig. 5(a)	$-0.327692\alpha^2$	$-0.19284\alpha^2$
Fig. 5(b)	$-0.188228\alpha^2$	$-0.11785\alpha^2$
Fig. 5(c)	$\frac{1}{2}\alpha^2$	$\frac{1}{3}\alpha^2$
Total	$+0.01592\alpha^2$	$0.02263\alpha^2$

TABLE II. Polaron ground-state energy $E_0/\hbar\Omega$ (in units of optical-phonon energies) as a function of coupling constant α .

$E_0/\hbar\Omega$	1	3	5	α 7	9	11	13
Lee and Pines ^a	-1.00	-3.10	-5.30	-7.58	-9.95	-12.41	
Feynman and Schultz ^a	-1.01	-3.13	-5.44	-8.11	-11.49	-15.71	-20.60 ^b
$(E_0/\hbar\Omega)_{\text{Feyn}}$	-1.01	-3.16	-5.65	-8.67	-12.33	-16.72	-21.89
$(E_0/\hbar\Omega)_{\text{pert}}$	-1.02	-3.33	-6.14	-9.59	-13.74	-18.65	-24.33

^aT. D. Schultz, Phys. Rev. 116, 526 (1959).^bValue calculated by author.

leigh-Schrödinger perturbation theory: The result, which is proportional to α^2 , is displayed in Fig. 10 for $\alpha = 1$, and diverges as $(k_0^2 - k^2)^{-1/2}$ as k approaches $k_0 = (2m\Omega/\hbar)^{1/2}$. This divergence is, once more, perturbation theory's way of telling us that it is unable to describe the region near the phonon-emission threshold.

An approximation which should yield the correct threshold behavior is the Tamm-Dancoff method—a variational determination of the ground-state energy (for given momentum), using a trial wave function which includes only the zero- and one-phonon states of the lattice field.⁴³ The Tamm-Dancoff dispersion formula is

$$E(\alpha, k) = \frac{\hbar^2 k^2}{2m} - \frac{\alpha \hbar \Omega}{k(\hbar/2m\Omega)^{1/2}} \times \tan^{-1} \frac{k(\hbar/2m\Omega)^{1/2}}{[\hbar\Omega - E(\alpha, k)]^{1/2}}. \quad (4.2)$$

Since the Tamm-Dancoff approximation solves the zero- and one-phonon problem exactly, it should provide the proper description of the dispersion curve near threshold, even for intermediate and large values of α . Note that the cusp and divergence of second- and fourth-order perturbation theory are replaced by a more plausible threshold behavior ($dE/dk \rightarrow 0$) with this approximation. However, the Tamm-Dancoff result has two major drawbacks: (i) It fails to shift the one-phonon

emission energy down to $\hbar\Omega$ above the ground state [i. e., the threshold energy is $E(\alpha, 0) = -|E(\alpha, 0)|$; thus the energy required to emit one phonon is $\hbar\Omega + |E(\alpha, 0)|$ and not $\hbar\Omega$]. (ii) It predicts weak-coupling ground-state energies and effective masses which are correct only in lowest order (α); the α^2 corrections to the energy and the effective mass have the wrong sign.⁴³

The reason for the failure of Tamm-Dancoff theory is its omission of many-phonon states. This may be seen by the following qualitative arguments. First consider a static electron interacting with the optical phonons of an insulating solid. Each ion will feel an extra force due to the extra charge and will therefore have an equilibrium position displaced somewhat from its lattice site (its equilibrium position in the absence of the extra electron). The effect of this displacement will be to lower the ground-state energy of the lattice vibrations and to shift their equilibrium positions. Such a shift of ionic equilibrium positions necessarily involves an infinite number of perfect-lattice phonons since the shifted state is qualitatively different from the unperturbed state. These ideas are demonstrated qualitatively by considering a single charged oscillator of mass M and frequency Ω , subjected to an interaction with the conduction-band electron:

$$H = P^2/2M + \frac{1}{2}M\Omega^2 X^2 + \lambda X + \sigma. \quad (4.3a)$$

The electron-oscillator interaction is taken to be linear in the displacement of the oscillator; the electrostatic interaction energy of the electron and the equilibrium oscillator is represented by σ , and the energy due to displacement in the presence of the electron is λX . The "electric field" λ plays a role similar to $\alpha^{1/2}$ in the polaron Hamiltonian. The oscillator Hamiltonian (4.3a) is easily rewritten as

$$H = P^2/2M + \frac{1}{2}M\Omega^2(X + \lambda M^{-1}\Omega^{-2})^2 - \frac{1}{2}M^{-1}\Omega^{-2}\lambda^2 + \sigma. \quad (4.3b)$$

Note that the energy eigenstates are still separated by $\hbar\Omega$, but all of the states are shifted to lower en-

TABLE III. Polaron effective mass m^*/m (in units of the electron band mass) as a function of coupling constant α .

m^*/m	α					
	1	3	5	7	9	11
Lee and Pines ^a	1.19	1.61	2.15	2.82	3.58	4.4
Feynman and Schultz ^a		1.89	3.89	14.4	62.5	185
$(m^*/m)_{\text{Feyn}}$	1.19	1.95	6.44	26.47	84.03	210.05
$(m^*/m)_{\text{pert}}$	1.17	1.78	5.99	25.72	83.01	208.82
Pekar, Bugoliubov, and Tyablikov ^a		14	55.7	152	340	

^aT. D. Schultz, Phys. Rev. 116, 526 (1959).

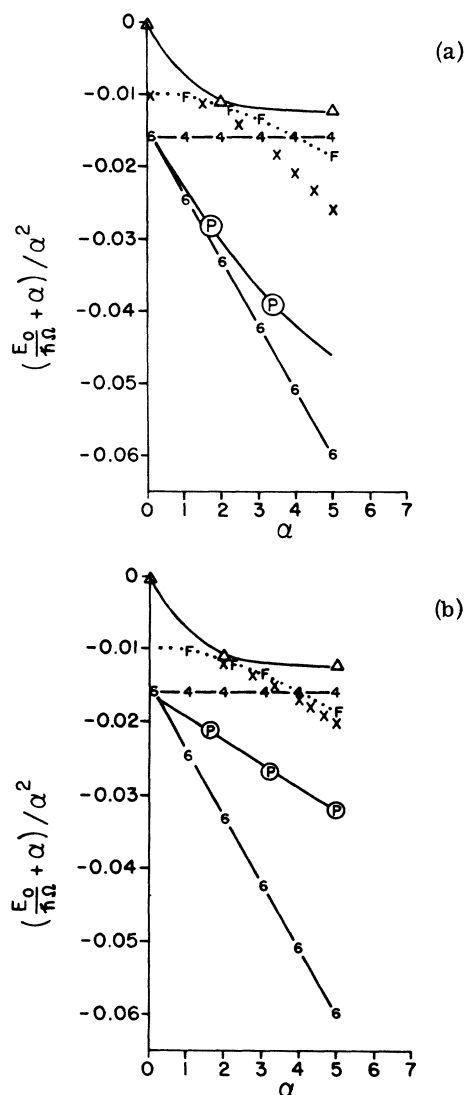


FIG. 8. (a) Polaron ground-state energy as a function of coupling constant α plotted on an expanded scale. The notation here is the same as in Fig. 6. Note that the [2, 4] Padé approximant about 0 and ∞ is better than Feynman's result at weak coupling. (b) Polaron ground-state energy as a function of coupling constant plotted on an expanded scale. The symbols have the same meanings as in Fig. 6. The two-point Padé approximants are fitted about $\alpha = 0$ and $\alpha = 20$. Note that (i) the Padé approximant to Feynman's calculation is extremely accurate; and (ii) the Padé approximant to the weak-coupling perturbation theory and the strong-coupling variational calculation is better than Feynman's theory in these regimes.

ergy by the same amount, proportional to λ^2 —leading us to anticipate that in the polaron problem the phonon continua will all shift (linearly with α for small α) to lower energy. Hence, the presence of a static electron causes a many-phonon dis-

placement of the equilibrium positions for the ions in the crystal. Now consider a slowly moving electron. It will also cause the ions to vibrate about displaced equilibrium sites, with the amount of displacement somewhat dependent on the velocity of the electron. It follows that an accurate treatment of the electron-phonon interaction must include the (velocity-dependent) displacement of the ions caused by the electron. Any perturbation treatment which does not include this physical displacement is doomed to convergence difficulties. Thus, even the variational (one-phonon) Tamm-Dancoff method fails to obtain the correct phonon-excitation energy because it does not account for the many-phonon continuum shifts associated with the displaced oscillators.

This physical situation of continuum shifts and displaced oscillators is hinted at mathematically by the behavior of the polaron energy levels in perturbation theory. Consider a slow electron of wave vector \vec{k} interacting with the phonons. By momentum conservation, it only interacts with N one-phonon states (N is the number of unit cells in the crystal), namely those with an electron of wave vector $\vec{k} - \vec{q}$ and a phonon of wave vector \vec{q} for all N values of \vec{q} . The effect of this interaction is to push the one-electron zero-phonon state down in energy while pushing the one-electron one-phonon states up (i. e., the states repel). There are N^2 two-phonon states (phonons of wave vectors \vec{q}_1

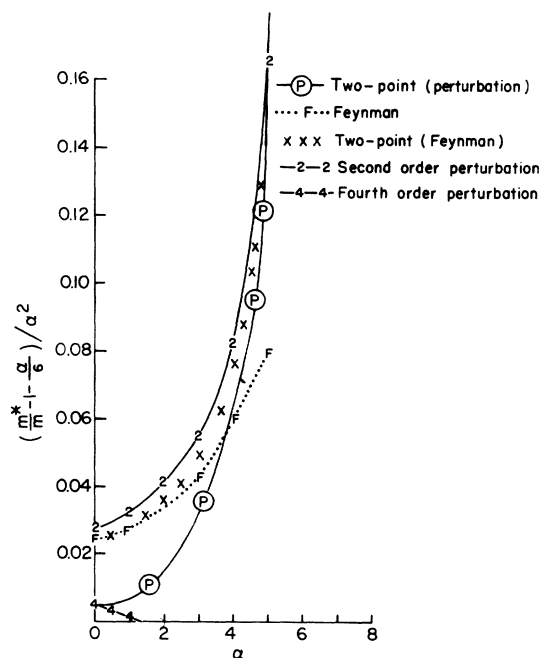


FIG. 9. Polaron effective mass as a function of coupling constant α plotted on an expanded scale. The notation here is the same as in Fig. 6.

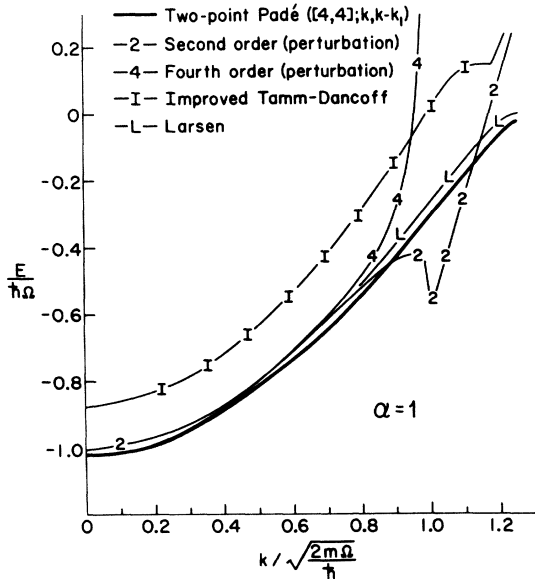


FIG. 10. Polaron-dispersion relation plotted as a function of wave vector for coupling constant $\alpha=1$. The solid lines with 2 and 4 denote the second- and fourth-order perturbation calculations. The heavy solid line denotes the two-point Padé approximant. The lines with L and I represent the Larsen (see Ref. 13) and the improved Tamm-Dancoff (see Ref. 32) calculations, respectively. Note that the Padé approximant curve has the same general shape as Larsen's curve but gives a lower energy.

and \vec{q}_2 and an electron of wave vector $\vec{k} - \vec{q}_1 - \vec{q}_2$ which also push the zero-phonon state down, and are pushed up in return. These two-phonon states also push the one-phonon states down in energy. In general, for a given polaron wave vector \vec{k} , there are N^n n -phonon states pushing the lowest polaron energy down (by an amount proportional to α^n), and also pushing the energies of the $n-1$, $n-2, \dots$ phonon states to lower energy as well. Now a calculation of the polaron-dispersion curve (such as the Tamm-Dancoff calculation) which includes only one-phonon states should appropriately depress the energies of the different zero-phonon unperturbed states, but the threshold for phonon emission should lie at too high an energy (because two- and more-phonon states have not been included to push the one-phonon states down).

Still, the Tamm-Dancoff approximation does account for the strong mixing of zero- and one-phonon states near the emission threshold, and therefore can be expected to give the correct shape of $E(\vec{k})$ near threshold (at least for weak electron-phonon coupling α and for states whose energies differ from the threshold energy by much less than $\hbar\Omega$).

The above discussion suggests that a simple but

accurate method for obtaining the weak-coupling polaron-dispersion relation is to first displace the normal modes of the lattice (using the displaced-oscillator transformation of Lee, Low, and Pines) and then to evaluate the ground-state energy using a variational Tamm-Dancoff-type approximation. Such a procedure was used by Larsen, and did result in an improved dispersion relation with a one-phonon threshold $\hbar\Omega$ above the ground state.¹³ The Larsen approximation is almost certainly the best available in the spectral region near threshold. The main disadvantage of Larsen's method is that it requires numerical evaluation of the dispersion curve. Therefore we shall only use the Larsen method to obtain the value k_1 of the wave vector of the phonon-emission threshold; information about the shape of the dispersion curve near threshold will be gotten from the Tamm-Dancoff approximation itself.

In addition to the Tamm-Dancoff approximation, there is the Whitfield-Puff improved Tamm-Dancoff approximation which overcomes the first Tamm-Dancoff difficulty by summing the nested diagrams (Fig. 4) in order to get a polaron self-energy with a phonon-emission threshold exactly $\hbar\Omega$ above the ground state.⁴⁴ However, the Whitfield-Puff approximation fails to obtain a sufficiently low ground-state energy (see Fig. 10) or a sufficiently accurate effective mass, presumably because the crossing diagrams (Fig. 5) have been omitted. And finally, evaluation of the Whitfield-Puff dispersion relation requires the numerical solution of Pines's equation⁴⁵ (Figs. 2 and 4); in view of the drawbacks of the Whitfield-Puff solution, we do not use it in formulating an optimal dispersion relation. The strong-coupling theories generally have not produced complete dispersion relations and therefore provide little useful information about the dependence of the strong-coupling energy on k . It follows that the "best" dispersion relation which we construct using Padé approximants will be quite accurate if $\alpha \lesssim 1$, but of limited utility for $\alpha \gg 1$. The various approximations to the polaron-dispersion curve, their ranges of validity, and their good and bad features are summarized in Table IV.

In order to evaluate a "best" dispersion relation which incorporates the good features of the various approximations while discarding the bad features, we assume the following: (a) Near the phonon-emission threshold, the shape of the dispersion curve is given adequately by the Tamm-Dancoff approximation; (b) near $k=0$ perturbation theory is valid for small α ; (c) the energy of the one-phonon emission threshold must lie exactly $\hbar\Omega$ above the ground state; and (d) the threshold wave vector is adequately given by Larsen's method (Fig. 11). All four of these assumptions are consistent with the general results of Cannon⁴⁶: (i) $E(\alpha, k)$ for any fixed value

TABLE IV. Approximations used for obtaining the (nonparabolic) polaron-dispersion relation $E(\alpha, k)$ together with their good and bad features.

Approximation	Good features	Bad features
Second-order perturbation theory	Valid for $\alpha \ll 1$ and $k \ll (2m\Omega/\hbar)^{1/2}$	Cusp in $E(\alpha, k)$ at $k = (2m\Omega/\hbar)^{1/2}$. m^* , E_0 , and $E(\alpha, k)$ poorly given for $\alpha \gtrsim 1$.
Fourth-order perturbation theory	Valid for $\alpha \ll 1$ and $k \ll (2m\Omega/\hbar)^{1/2}$	Divergence in $E(\alpha, k)$ at $k = (2m\Omega/\hbar)^{1/2}$. m^* , E_0 , and $E(\alpha, k)$ poorly given for $\alpha \gtrsim 1$. $E(\alpha, k)$ must be evaluated numerically.
Sixth-order perturbation theory	Valid for $\alpha \ll 1$ and $k \ll (2m\Omega/\hbar)^{1/2}$	Only E_0 can be easily calculated (numerically). E_0 poorly given for $\alpha \gtrsim 1$.
Tamm-Dancoff	Variational theory, correct threshold behavior	E_0 and m^* are worse than second-order perturbation results; one-phonon emission threshold does not lie $\hbar\Omega$ above ground state.
Improved Tamm-Dancoff	Self-consistent theory, correct threshold behavior. Many-phonon states included. One-phonon threshold lies $\hbar\Omega$ above ground state.	m^* seems to be poorly given. E_0 is not low enough. Numerical solution of integral equation required.
Larsen	Displaced-oscillator transformation plus Tamm-Dancoff variational trial wave function. Correct threshold behavior. One-phonon threshold lies $\hbar\Omega$ above ground state.	Numerical integration required. E_0 , m^* poorly given for $\alpha \gtrsim 1$. $E(\alpha, k)$ good only for $\alpha \lesssim 3$.

of α is an analytic function of k for all k such that $E(k) < \hbar\Omega + E(0)$; (ii) $E(\alpha, k)$ is analytic in α for small α ; and (iii) $E(\alpha, k)$ merges into the continuum (it does not just approach the continuum asymptotically).

With these four assumptions, we shall evaluate the polaron-dispersion relation using a weak-coupling ($\alpha \ll 1$) two-point Padé approximant method which fits the perturbation results⁴⁷ (to order k^4) near $k=0$ and replicates the Tamm-Dancoff behavior [to order $(k-k_1)^3$] near the threshold wave vector k_1 . The requirements which the two-point Padé approximant (in k) must satisfy are

$$E(\alpha, k) = \tilde{E}_0(\alpha) + \frac{\hbar^2}{2m^*(\alpha)} k^2 + \frac{1}{4!} \frac{\partial^4 E}{\partial k^4} k^4 + O(k^6), \quad (4.4)$$

where $\tilde{E}_0(\alpha)$ and $m^*(\alpha)$ are the Padé approximants (in α) given in Eqs. (3.11) and (3.12), respectively, and $\partial^4 E / \partial k^4$ is given by second-order perturbation theory,

$$\frac{1}{4!} \frac{\partial^4 E}{\partial k^4} = -\alpha \left(\frac{\hbar^3}{m^2 \Omega} \right) \frac{3}{160}. \quad (4.5)$$

The expansion around k_1 is given by Tamm-Dancoff theory,

$$E(\alpha, k) = \hbar\Omega + E(\alpha, 0) + c_2(\alpha) \frac{(k-k_1)^2}{2!} + c_3(\alpha) \frac{(k-k_1)^3}{3!}, \quad (4.6)$$

where c_2 and c_3 are given in Appendix C. Equations (4.4) and (4.6) determine the [4, 4] two-point Padé approximant to $E(\alpha, k)$ [See Eq. (C1)]:

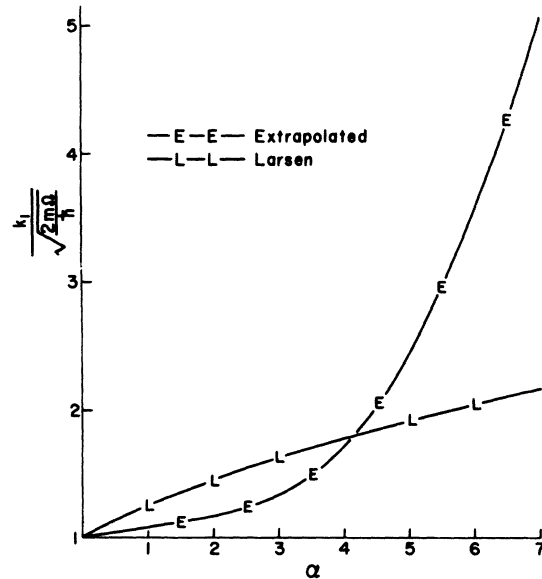


FIG. 11. Threshold wave vector as a function of polaron coupling constant α . The solid line with E denotes the values of threshold wave vector obtained by assuming a perfect parabola for the polaron-dispersion relation. The solid line with L denotes the values of threshold wave vector obtained from Larsen's theory (see Ref. 13).

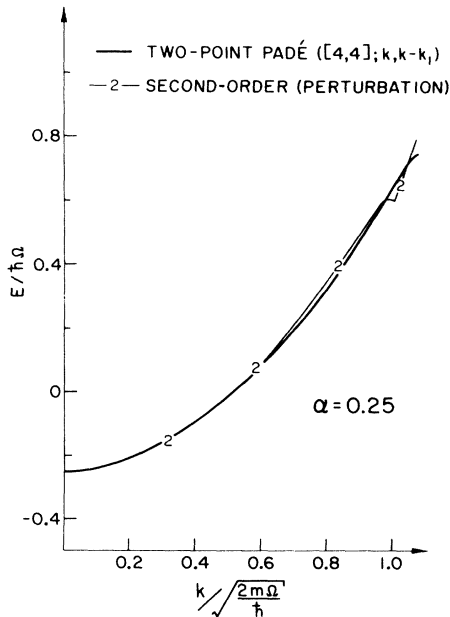


FIG. 12. Polaron-dispersion relation for coupling constant $\alpha = 0.25$. The notation is the same as in Fig. 10.

$$Q_{E(\alpha, k)}([4, 4], k, k - k_1),$$

which is plotted in Figs. 10, 12, and 13 for $\alpha = 1.0$, $\alpha = 0.25$, and $\alpha = 4.0$, respectively.

V. SUMMARY

The principal conclusion of this work is that relatively low-order weak- and strong-coupling expansions can be combined by the two-point Padé approximant method, giving a simple and amazingly-accurate intermediate-coupling theory. The two-point Padé method describes the ground-state energy and the effective mass of the polaron extremely well, and the Padé approximant to the polaron mass indicates that it is a continuous function of the coupling constant α . Therefore electron self-trapping via the electron-optical-phonon interaction should not occur.⁴²

In addition, the perturbation calculations of the polaron ground-state energy and effective mass have been extended to sixth and fourth order in $\alpha^{1/2}$, respectively. And finally we have speculated about the nature of the polaron-dispersion relation $E(\alpha, k)$ and have presented a simple description of it (which should be accurate for $\alpha \leq 1$) in terms of two-point Padé approximants.

In closing we would like to suggest lines which future research on two-point Padé approximants may fruitfully follow. First, two-point Padé methods should be applied to more problems in physics, so that it will be possible to anticipate when the

methods will work and when they will fail. And finally, there is very little known about the formal properties of either one- or two-point Padé approximants; in view of their phenomenal utility, a detailed study of their formal mathematical properties is definitely called for.

ACKNOWLEDGMENTS

We gratefully acknowledge helpful conversations with F. C. Weinstein, John J. Hopfield, and Arthur Wightman. We especially wish to thank Dr. Weinstein for checking the perturbation calculations. We are also grateful to G. Yuval for suggestions leading to an improved presentation of the material at the end of Sec. II and to B. Simon whose studies of Padé methods rekindled our interest in this problem.

APPENDIX A: TWO-POINT PADE APPROXIMANT TO $\tan Z$

In this appendix we fit

$$Q_{\tan}([4, 5]; Z, Z - 2\pi)$$

$$= Z \frac{a_0 + a_1 Z + a_2 Z^2 + a_3 Z^3 + a_4 Z^4}{1 + b_1 Z + b_2 Z^2 + b_3 Z^3 + b_4 Z^4} \quad (A1)$$

to $\tan Z$, using the power-series expansions about $Z = 0$ and $Z = 2\pi$:

$$\tan Z = Z + \frac{1}{3}Z^3 + \frac{2}{15}Z^5 + O(Z^7), \quad (A2a)$$

$$\tan Z = (Z - 2\pi) + \frac{1}{3}(Z - 2\pi)^3 + O((Z - 2\pi)^5). \quad (A2b)$$

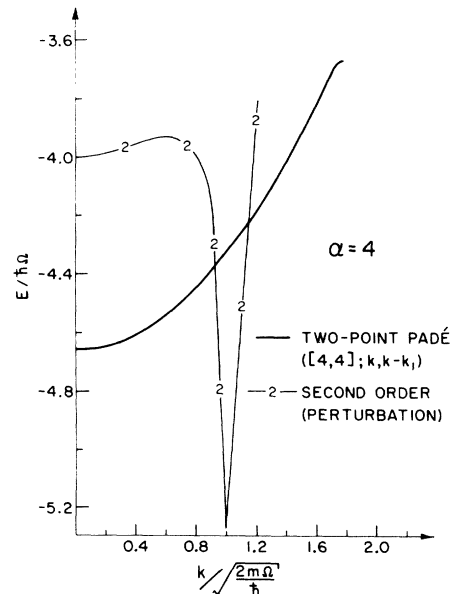


FIG. 13. Polaron-dispersion relation for coupling constant $\alpha = 4$. The notation here is the same as in Fig. 10.

Expanding Eqs. (A2a) and (A2b) about $Z=0$ and equating coefficients of the first five powers of Z [in a manner analogous to Eq. (2.13)], we obtain

$$a_0 = 1, \quad (\text{A3a})$$

$$a_1 - b_1 = 0, \quad (\text{A3b})$$

$$a_2 - b_2 = \frac{1}{3}, \quad (\text{A3c})$$

$$a_3 - \frac{1}{3}b_1 - b_3 = 0, \quad (\text{A3d})$$

$$a_4 - \frac{1}{3}b_2 - b_4 = \frac{2}{15}. \quad (\text{A3e})$$

Similar expansions about $Z=2\pi$ generate the remaining four equations for the a 's and b 's by equating the coefficients of equal powers of $(Z-Z_0)$ up to third order:

$$Z_0 a_1 + Z_0^2 a_2 + Z_0^3 a_3 + Z_0^4 a_4 = -1, \quad (\text{A3f})$$

$$2Z_0 a_1 + 3Z_0^2 a_2 + 4Z_0^3 a_3 + 5Z_0^4 a_4 - Z_0 b_1 - Z_0^2 b_2 - Z_0^3 b_3 - Z_0^4 b_4 = 0, \quad (\text{A3g})$$

$$2a_1 + 6Z_0 a_2 + 12Z_0^2 a_3 + 20Z_0^3 a_4 - 2b_1 - 4Z_0 b_2 - 6Z_0^2 b_3 - 8Z_0^3 b_4 = 0, \quad (\text{A3h})$$

$$6a_2 + 24Z_0 a_3 + 60Z_0^2 a_4 - 2Z_0 b_1 - 2(3+Z_0^2)b_2 - 2Z_0(9+Z_0^2)b_3 - 2Z_0^2(18+Z_0^2)b_4 = 0. \quad (\text{A3i})$$

These equations are linear in the a 's and b 's, and can be solved giving

$$Q_{\tan}([4, 5]; Z, Z-2\pi) = Z \frac{1 - 0.3575Z - 0.0371Z^2 + 0.0187Z^3 - 0.0012Z^4}{1 - 0.3575Z - 0.3704Z^2 + 0.1378Z^3 - 0.0111Z^4}. \quad (\text{A4})$$

This result is plotted and compared with the one-point Padé approximant of the same order, $P_{\tan}([2, 2]; Z^2)$, in Fig. 1.

APPENDIX B: FOURTH- AND SIXTH-ORDER PERTURBATION THEORY

Fourth Order

The fourth-order contribution to the ground-state energy is

$$E_k^{(4)} = -E_k^{(2)} \sum_{j \neq k} \frac{|H_1|_{jk}^2}{(E_k - E_j)^2} + \sum_{m \neq k} \sum_{j \neq k} \sum_{m \neq k} \frac{(H_1)_{jn}(H_1)_{kj}(H_1)_{nm}(H_1)_{mk}}{(E_k - E_j)(E_k - E_m)(E_k - E_n)}. \quad (\text{B1})$$

Here $E_k^{(2)}$ and E_k are the second-order and unperturbed energies of the state with wave vector \vec{k} , respectively. The contributions to $E_k^{(4)}$ correspond to the diagrams of Fig. 5. For $\vec{k}=0$ these diagrams reduce to

$$\text{Figure 5(a): } -\frac{1}{\pi^2} \alpha^2 \hbar \Omega \int_0^\infty dq \int_0^\infty dq' \frac{1}{qq'(1+q^2)^2} \ln \left(\frac{2+(q+q')^2}{2+(q-q')^2} \right) = -0.327692 \alpha^2 \hbar \Omega; \quad (\text{B2a})$$

$$\text{Figure 5(b): } -\frac{1}{\pi^2} \alpha^2 \hbar \Omega \int_0^\infty dq \int_0^\infty dq' \frac{1}{qq'(1+q^2)(1+q'^2)} \ln \left(\frac{2+(q+q')^2}{2+(q-q')^2} \right) = -0.188228 \alpha^2 \hbar \Omega; \quad (\text{B2b})$$

$$\text{Figure 5(c): } \frac{1}{2} \alpha^2 \hbar \Omega. \quad (\text{B2c})$$

The contributions of these same diagrams to the inverse effective mass is obtained from the coefficient of the k^2 term of $E_k^{(4)}$ for k near zero. The contributions to m/m^* are

$$\begin{aligned} \text{Figure 5(a): } & -\frac{8}{3\pi^2} \alpha^2 \int_0^\infty \int_0^\infty dq dq' \frac{\frac{1}{2} + 2q^2}{(1+q^2)^4 qq'} \ln \left(\frac{2+(q+q')^2}{2+(q-q')^2} \right) - \frac{32\alpha^2}{3\pi^2} \int_0^\infty \int_0^\infty dq dq' \frac{1}{(1+q^2)} J(q, q') \\ & = -0.19284 \alpha^2, \quad (\text{B3a}) \end{aligned}$$

$$\begin{aligned} \text{Figure 5(b): } & -\alpha^2 \left\{ \frac{1}{6} + \frac{8}{3\pi^2} \int_0^\infty \int_0^\infty dq dq' \left[\frac{1}{2(1+q^2)} + \frac{q^2}{(1+q^2)^2} - \frac{2+q^2+q'^2}{4(1+q^2)(1+q'^2)} \right] \frac{1}{(1+q^2)(1+q'^2)qq'} \right. \\ & \quad \left. \times \ln \left(\frac{2+(q+q')^2}{2+(q-q')^2} \right) \right\} - \frac{32\alpha^2}{3\pi^2} \int_0^\infty \int_0^\infty dq dq' \frac{1}{(1+q^2)} J(q, q') = -0.11785 \alpha^2, \quad (\text{B3b}) \end{aligned}$$

Figure 5(c): $\frac{1}{3}\alpha^2$.

(B3c)

Here we have

$$J(q, q') = \frac{\frac{1}{2}(q^2 - q'^2 - 2)}{(1+q^2)^2 [4(1+q^2+q'^2) + (q^2 - q'^2)^2]} + \frac{q^2(1+q^2)(2+q^2 - q'^2)}{[4(1+q^2+q'^2) + (q^2 - q'^2)^2](1+q^2)^2}. \quad (\text{B4})$$

Sixth Order

The sixth-order contribution to the ground-state energy is

$$E_k^{(6)} = (E_k^{(2)})^2 \sum_{j \neq k} \frac{|H_1|_{jk}^2}{(E_k - E_j)^3} - 2E_k^{(2)} \sum_{\substack{j \neq k \\ n \neq k \\ m \neq k}} \frac{(H_1)_{kj}(H_1)_{jn}(H_1)_{nm}(H_1)_{mk}}{(E_k - E_m)(E_k - E_j)^2(E_k - E_n)} - E_k^{(2)} \sum_{\substack{j \neq k \\ n \neq k \\ m \neq k}} \frac{(H_1)_{kj}(H_1)_{jn}(H_1)_{nl}(H_1)_{lk}}{(E_k - E_l)(E_k - E_n)^2(E_k - E_j)} \\ + \sum_{j, n, m, l, i \neq k} \frac{(H_1)_{kj}(H_1)_{jn}(H_1)_{nm}(H_1)_{mi}(H_1)_{li}(H_1)_{ik}}{(E_k - E_m)(E_k - E_n)(E_k - E_j)(E_k - E_l)(E_k - E_i)}. \quad (\text{B5})$$

The last term in the summation can be split into the eight distinctive contributions represented by the diagrams of Fig. 14(a)–(h). Each diagram corresponds to a different energy denominator. For example, for $k=0$, Figure 14(c) corresponds to the integral

$$-\frac{\hbar\Omega\alpha^3}{8\pi^6} \int \int \int \int \int \int dq_1 dq_2 dq_3 d\Omega_1 d\Omega_2 d\Omega_3 \frac{1}{(1+q_1^2)(1+q_2^2)(1+q_3^2)[2+(\bar{q}_1+\bar{q}_2)^2][2+(\bar{q}_2+\bar{q}_3)^2]}.$$

Some (but not all) of these integrals can be simplified. For example, Fig. 14(a) can be simplified to

$$-\frac{\hbar\Omega\alpha^3}{2\pi^3} \int_0^\infty \frac{dq}{(1+q^2)^3} [F(q)]^2, \quad \times \left[1 + \sum_{n=1}^\infty \left(\frac{q^2}{3+q^2} \right)^n \frac{[(2n-1)!!]^2}{(2n+1)!} \right];$$

where

$$F(q) = \frac{2\pi}{(3+q^2)^{1/2}}$$

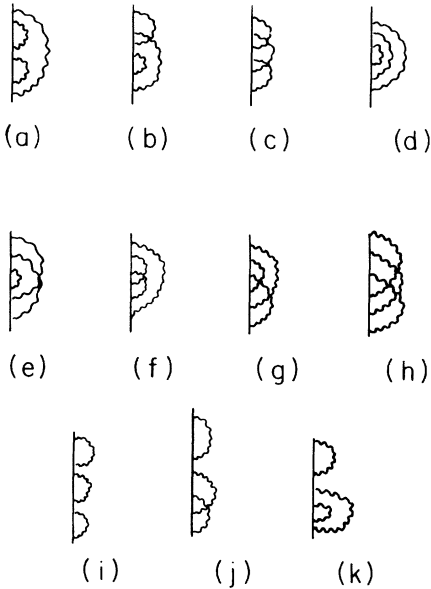


FIG. 14. Diagrams contributing to the polaron energy in sixth-order perturbation theory. The wiggly line represents the free-phonon propagator and the straight line represents the free-electron propagator.

Fig. 14(b) reduces to

$$-\frac{\hbar\Omega\alpha^3}{2\pi^3} \int_0^\infty \frac{dq}{(1+q^2)^2} F(q) \times \left[\int_0^\infty \frac{dx}{(1+x^2)xq} \ln \left(\frac{2+(x+q)^2}{2+(x-q)^2} \right) \right].$$

The contributions of the various diagrams are listed in Table V.

APPENDIX C: TWO-POINT PADÉ APPROXIMANT TO $E(k)$

The Padé approximant in this case is obtained using all the derivatives up to third order of the Tamm-Dancoff dispersion relation near the threshold and the perturbation expansion up to k^4 near $k=0$. Let us denote the first, second, and third derivatives (evaluated at threshold) with respect to k of the Tamm-Dancoff energy by c_1 , c_2 , and c_3 , respectively. The coefficient of k^2 is denoted by E_1 and coefficient of k^4 by E_2 . Then the $[4, 4]$ Padé will have the form

$$\sum_{i=0}^4 a_i k^i / \sum_{i=0}^4 b_i k^i, \quad (\text{C1})$$

where all k 's are measured in units of $(2m\Omega/\hbar)^{1/2}$, and all energies are in units of $\hbar\Omega$. Using the methods of Appendix A, we have

$$a_0 = E(0), \quad (\text{C2a})$$

TABLE V. Sixth-order perturbation contribution to the polaron ground-state energy E_0 .

Fig. 14	Weight of contribution	Contribution of diagram to $E_0/\hbar\Omega$ times weight
(a)	1	$-0.1733610504\alpha^3$
(b)	2	$-0.17093505450\alpha^3$
(c)	1	$-0.04516594437\alpha^3$
(d)	1	$-0.03761305677\alpha^3$
(e)	1	$-0.03225926949\alpha^3$
(f)	1	$-0.02288236116\alpha^3$
(g)	2	$-0.03448518772\alpha^3$
(h)	1	$-0.01501993833\alpha^3$
(i)	1	$-\frac{3}{8}\alpha^3$
(j) and (k)	1	$0.8979561338\alpha^3$
Total		$-0.008765\alpha^3$

$$b_0 = 1, \quad (\text{C2b})$$

$$b_4 = (K_1 M_3 - K_3 M_1) / (K_1 M_2 - K_2 M_1), \quad (\text{C2c})$$

$$b_2 = (M_3 - M_2 b_4) / M_1, \quad (\text{C2d})$$

$$b_1 = \frac{1}{2} [k_1 E_1 - 3/k_0 - k_1^3 E_2 + k_1^3 b_4 - (k_1^3 E_1 + k_1) b_2], \quad (\text{C2e})$$

$$b_3 = [(k_1^2 E_1 - 1)(k_1 b_1 + k_1^2 b_2) - k_1^4 b_4 - 1 + k_1^2 (E_1 + k_1^2 E_2)] / k_1^3, \quad (\text{C2f})$$

$$a_1 = E(0) b_1, \quad (\text{C2g})$$

$$a_2 = E_1 + E(0) b_2, \quad (\text{C2h})$$

$$a_3 = E(0) b_3 + E_1 b_1, \quad (\text{C2i})$$

and

$$a_4 = E_2 + E(0) b_4 + E_1 b_2, \quad (\text{C2j})$$

where

$$K_1 = (1 + 3k_1^2 E_1) + \frac{1}{2} c_2 k_1^4 E_1 (k_1^2 E_1 - 1),$$

$$K_2 = -13 k_1^2 + \frac{1}{2} c_2 k_1^4 E_1,$$

$$K_3 = \frac{3}{2} (1 + k_1^2 E_1) / k_1^2 - \frac{7}{2} E_2 k_1^2 + \frac{1}{2} c_2 [1 + \frac{1}{8} k_1^2 E_1 (1 + 3E_1 k_1^2) + E_2 k_1^4 (\frac{7}{3} - \frac{1}{2} E_1 k_1^2)],$$

$$M_1 = (3/k_1) (1 + 5k_1^2 E_1) + \frac{3}{2} c_2 E_1 k_1^3 (3k_1^2 E_1 - 5) + \frac{1}{2} c_3 E_1 k_1^4 (k_1^2 E_1 - 1),$$

$$M_2 = -k_1 (15 + \frac{9}{2} c_2 E_1 k_1^4 + \frac{1}{2} c_3 E_1 k_1^5)$$

$$M_3 = 3 \left(\frac{1}{k_1^3} - 5k_1 E_2 \right) + 3E_1 \left(\frac{1}{k_1} - \frac{1}{2} k_1^2 \right)$$

$$+ \frac{3}{2} c_2 E_1 k_1 (3k_1^2 E_1)$$

$$+ \frac{3}{2} c_2 E_2 k_1^3 (8 - 3k_1^2 E_1) + \frac{1}{2} c_3 E_1 k_1^2 (2 + k_1^2 E_1) + \frac{1}{2} c_3 E_2 k_1^4 (2 - k_1^2 E_1),$$

$$c_1 = 0,$$

$$c_2 = -2 \left(\frac{3}{2} \pi + 2x/\alpha \right)^2,$$

and

$$c_3 = (-12x^3/\alpha^2) (3x^2 - 1) [3 + (\frac{3}{2} \pi + 2x/\alpha)^2] - (12/x) (\frac{3}{2} \pi + 2x/\alpha)^2.$$

Here x is the real root of the equation $x^3 - x - \frac{1}{2} \alpha \pi = 0$ and k_1 is the threshold wave vector.

*Work supported by the Air Force Office of Scientific Research under Contract No. AF49(638)1545.

†Gulf Oil Predoctoral Fellow. Present address: Institute for Advanced Study, Princeton, N. J. 08540.

‡Work supported in part by the National Science Foundation.

¹H. Fröhlich, H. Pelzer, and S. Zienau, *Phil. Mag.* **41**, 221 (1950).

²For a review of polaron theory, see J. Appel, *Solid State Phys.* **21**, 193 (1968).

³G. R. Allcock, *Advan. Phys.* **5**, 412 (1956).

⁴G. A. Baker, Jr., *Advances in Theoretical Physics* (Academic, New York, 1968), Vol. 1, p. 1.

⁵G. A. Baker, Jr., G. S. Rushbrooke, and H. E. Gilbert, *Phys. Rev.* **135**, A1272 (1964).

⁶P. Sheng and J. D. Dow, *Bull. Am. Phys. Soc.* **16**, 124 (1971); *Phys. Status Solidi* **44**, K131 (1971).

⁷G. Höhler and A. Mullensieffen, *Z. Physik* **157**, 159 (1959).

⁸S. I. Pekar, *Untersuchungen Über die Elektron Theorie der Kristalle* (Akademie-Verlag, Berlin, 1954) [English translation: *Research in Electron Theory of Crystals*, Division of Technical Information, U.S.

Atomic Energy Commission Report No. AEC-Tr-5575 (unpublished)].

⁹T. D. Lee, F. Low, and D. Pines, *Phys. Rev.* **90**, 297 (1953).

¹⁰T. D. Lee and D. Pines, *Phys. Rev.* **92**, 883 (1953).

¹¹W. van Haeringen, *Phys. Rev.* **137**, A1902 (1965).

¹²E. P. Gross, *Phys. Rev.* **100**, 1571 (1955).

¹³D. M. Larsen, *Phys. Rev.* **144**, 697 (1966).

¹⁴R. P. Feynman, *Phys. Rev.* **97**, 660 (1955).

¹⁵It has been shown that, for Stieltjes series, the $[N, N]$ and $[N, N-1]$ Padé approximants to the series are upper and lower bounds, respectively.

¹⁶For a review of Padé approximant theory, see Ref. 4; and G. A. Baker, Jr. and J. L. Gammel, *Padé Approximants in Theoretical Physics* (Academic, New York, 1970).

¹⁷V. J. Emery, J. L. Gammel, and F. R. A. Hopgood, *Phys. Rev.* **132**, 10 (1963).

¹⁸C. Lovelace and D. Masson, *Nuovo Cimento* **26**, 472 (1962).

¹⁹G. A. Baker, Jr., *Phys. Rev.* **124**, 768 (1961).

²⁰B. Simon, *Ann. Phys.* **58**, 76 (1970); J. J. Loeffel, A. Martin, B. Simon, and A. S. Wightman, *Phys. Lett.*

ters 30B, 656 (1969).

²¹K. T. Tang and M. Karplus, Phys. Rev. 171, 70 (1968).

²²A. C. Yates and P. W. Langhoff, Phys. Rev. Letters 25, 1317 (1970).

²³M. Yokota and O. Tanimoto, J. Phys. Soc. Japan 22, 779 (1967).

²⁴While Padé approximants often reproduce the poles of the approximated function quite well, not every pole of the Padé approximant is to be interpreted as an approximate pole of the function—only those poles which remain at approximately the same place for every order of Padé approximant are true poles of the function.

²⁵This is

$$Q_{\tan}([4, 5]; z, z - 2\pi)$$

$$= z \frac{1 - 0.3575z - 0.0371z^2 + 0.0187z^3 - 0.0012z^4}{1 - 0.3575z - 0.3704z^2 + 0.1378z^3 - 0.0111z^4}.$$

²⁶J. D. Dow, P. Sheng, and F. C. Weinstein (unpublished).

²⁷Many-point Padé approximants may eventually be used, for example, to calculate the variation of a particular atomic energy level as a function of applied magnetic field strength B . Perturbation expansions about $B=0$, $B=\infty$, and some values of B for which level crossings occur may be used to determine the energy for all field strengths.

²⁸G. A. Baker, Jr., Phys. Rev. 136, A1376 (1964).

²⁹P. Sheng (unpublished).

³⁰H. Fröhlich, Advan. Phys. 3, 325 (1954).

³¹E. Haga, Progr. Theoret. Phys. (Kyoto) 11, 449 (1954).

³²G. Whitfield and R. Puff, Phys. Rev. 139, A338 (1965).

³³M. Porsch and J. Roseler, Phys. Status Solidi 23, 365 (1967).

³⁴Our diagrammatic notation is the same as in D. Pines, in *Polarons and Excitons*, edited by C. G. Kuper and G. D. Whitfield (Plenum, New York, 1966), p. 155.

³⁵In fact the α^2 term in the Tamm-Dancoff expression for ground-state energy has the wrong sign (this has been shown in Ref. 9). The fourth-order (α^2) contribution of Tamm-Dancoff theory to the effective mass is also in disagreement with perturbation theory: $(E_0/\hbar\Omega) = -\alpha + 0.5\alpha^2$, $(m^*/m) = 1 + \frac{1}{6}\alpha - \frac{11}{36}\alpha^2$, compared with Eqs. (3.8) and (3.9).

³⁶This canonical transformation to displaced-oscillator coordinates permits the elimination of the electron's coordinates from the problem.

³⁷The strong-coupling results can be obtained by a straightforward variational method (see Ref. 3).

³⁸Feynman's expression for the ground-state energy is

$$\frac{E_0}{\hbar\Omega} = \frac{3(v-w)^2}{4v} - \frac{\alpha\omega}{\pi^{1/2}v} \int_0^\infty \frac{e^{-t}d\tau}{\mathcal{K}(\tau)}.$$

The effective-mass formula is

$$\frac{m^*}{m} = 1 + \frac{\alpha}{3\pi^{1/2}} \left(\frac{v}{w}\right)^3 \int_0^\infty \frac{e^{-\tau}\tau^2}{[\mathcal{K}(\tau)]^3} d\tau,$$

where $\mathcal{K}(\tau) = \{\tau + [(v^2 - w^2)/vw^2](1 - e^{-v\tau})\}^{1/2}$.

The parameters v and w are determined by the variational condition $\partial E_0/\partial v = 0 = \partial E_0/\partial w$.

³⁹The coefficient of α^2 for m/m^* differs from the value of 0.0042 calculated in Ref. 7.

⁴⁰N. N. Bogoliubov and S. W. Tyablikov, Zh. Eksperim. i Teor. Fiz. 19, 256 (1949); S. W. Tyablikov, *ibid.* 21, 377 (1951).

⁴¹This is

$$E_0([1, 3]; \alpha, \alpha - 20)$$

$$= \frac{-\alpha - 0.035592245\alpha^2 - 0.003793659\alpha^3}{1 + 0.019672245\alpha}.$$

^{41a}D. M. Larsen, Phys. Rev. 187, 1147 (1969).

⁴²Y. Toyozawa, in *Polarons and Excitons*, edited by C. G. Kuper and G. D. Whitfield (Plenum, New York, 1963), p. 211; Y. Toyozawa, Progr. Theoret. Phys. (Kyoto) 26, 29 (1961).

⁴³The variational Tamm-Dancoff approximation obtains a ground-state energy which exceeds the second-order perturbation result. This of itself is no cause for alarm (in general the second-order energy is not necessarily an upper bound of the ground-state energy). Still it has been shown by variational methods (Ref. 9) for the case of the polaron that the second-order energy ($-\alpha\hbar\Omega$) is an upper bound on the ground state. Tamm-Dancoff theory predicts $(E_0/\hbar\Omega) = -\alpha + \frac{1}{2}\alpha^2 + \dots$, $(m^*/m) = 1 + \frac{1}{6}\alpha - \frac{11}{36}\alpha^2 + \dots$.

⁴⁴It is perhaps remarkable that the nested diagrams alone can shift the one-phonon continuum down to $\hbar\Omega$ above the ground state.

⁴⁵Pines's equation is

$$\Sigma(\vec{p}, \epsilon) = \int \frac{d^3k}{(2\pi)^3} |V_k|^2 \frac{1}{\left(\epsilon - \frac{\hbar^2(\vec{p}-\vec{k})^2}{2m} - \hbar\Omega\right)} - \Sigma(\vec{p}-\vec{k}, \epsilon - \hbar\Omega) + i\delta$$

(see Ref. 34, p. 170).

⁴⁶J. J. Cannon, thesis (Princeton University, 1968) (unpublished).

⁴⁷The coefficients of the k^0 , k^2 , and k^4 terms are calculated to sixth, fourth, and second order in $\alpha^{1/2}$, respectively.